AMERICAN SOCIETY FOR MICROBIOLOGY | Journal of Virology

An Ebola Virus-Like Particle-Based Reporter System Enables Evaluation of Antiviral Drugs *In Vivo* under Non-Biosafety Level 4 Conditions

Dapeng Li, Tan Chen, Yang Hu, Yu Zhou, Qingwei Liu, Dongming Zhou, Xia Jin, Zhong Huang

Vaccine Research Center, CAS Key Laboratory of Molecular Virology and Immunology, Institut Pasteur of Shanghai, Shanghai Institutes for Biological Sciences, Chinese Academy of Sciences, Shanghai, China

ABSTRACT

Ebola virus (EBOV) is a highly contagious lethal pathogen. As a biosafety level 4 (BSL-4) agent, however, EBOV is restricted to costly BSL-4 laboratories for experimentation, thus significantly impeding the evaluation of EBOV vaccines and drugs. Here, we report an EBOV-like particle (EBOVLP)-based luciferase reporter system that enables the evaluation of anti-EBOV agents *in vitro* and *in vivo* outside BSL-4 facilities. Cotransfection of HEK293T cells with four plasmids encoding the proteins VP40, NP, and GP of EBOV and firefly luciferase (Fluc) resulted in the production of Fluc-containing filamentous particles that morphologically resemble authentic EBOV. The reporter EBOVLP was capable of delivering Fluc into various cultured cells in a GP-dependent manner and was recognized by a conformation-dependent anti-EBOV monoclonal antibody (MAb). Significantly, inoculation of mice with the reporter EBOVLP led to the delivery of Fluc protein into target cells and rapid generation of intense bioluminescence signals that could be blocked by the administration of EBOV neutralizing MAbs. This BSL-4-free reporter system should facilitate high-throughput screening for anti-EBOV drugs targeting viral entry and efficacy testing of candidate vaccines.

IMPORTANCE

Ebola virus (EBOV) researches have been limited to costly biosafety level 4 (BSL-4) facilities due to the lack of animal models independent of BSL-4 laboratories. In this study, we reveal that a firefly luciferase-bearing EBOV-like particle (EBOVLP) with typical filamentous EBOV morphology is capable of delivering the reporter protein into murine target cells both *in vitro* and *in vivo*. Moreover, we demonstrate that the reporter delivery can be inhibited both *in vitro* and *in vivo* by a known anti-EBOV protective monoclonal antibody, 13C6. Our work provides a BSL-4-free system that can facilitate the *in vivo* evaluation of anti-EBOV antibodies, drugs, and vaccines. The system may also be useful for mechanistic study of the viral entry process.

Ebola virus (EBOV) is one of the most virulent and lethal human pathogens known. It is responsible for the 2013-2015 Ebola epidemic in West Africa, the greatest outbreak in history (1, 2), in which more than 28,000 suspected cases had been reported and over 11,000 deaths had been recorded as of September 2015. Due to the high transmissibility and mortality associated with the virus and the growing globalization that may facilitate the rapid spread of the virus around the world, EBOV is now recognized as a major threat to global public health and social stability. Therefore, the development of vaccines and therapeutics against EBOV is urgently needed (3, 4). However, EBOV is a biosafety level 4 (BSL-4) pathogen (5). Handling of various infectious forms of EBOV, including clinical isolates (6, 7); mouse/guinea pig-adapted strains (7–9); and recombinant EBOVs expressing reporter proteins, such as green fluorescent protein (10) or firefly luciferase (Fluc) (11), is highly restricted and can be performed only in BSL-4 facilities, greatly impeding the development of vaccines and drugs against EBOV. Given that there are only approximately 30 operational BSL-4 laboratories distributed globally in a few countries (12), the establishment of a safe, robust, and easily reproducible *in vitro* and *in vivo* infection system independent of BSL-4 facilities will significantly advance the research and development of vaccines and drugs against EBOV.

To date, several *in vitro* systems have been established for studying EBOV outside BSL-4 laboratories. One is the lentivirus/retrovirus-based EBOV pseudovirus, which was assembled by displaying EBOV glycoprotein (GP) on lentiviral/retroviral core particles (13). A recombinant vesicular stomatitis virus (rVSV) encoding EBOV GP and green fluorescent protein (GFP) reporters has also been generated (14). However, lentiviral/retroviral particles and VSV particles are usually spherical and bullet shaped, respectively, and thus are morphologically different from the filamentous and pleomorphic EBOV particles. Previous studies have shown that coexpression of the EBOV matrix protein (VP40), nucleoprotein (NP), and GP in mammalian cells (15, 16) or insect cells (17) resulted in the assembly of EBOV-like particles (EBOVLP) that were morphologically similar to EBOV particles. Based on these observations, an EBOVLP with VP40 fused to β-lactamase was engineered and used for studying EBOV entry by

Received 26 June 2016 **Accepted** 13 July 2016

Accepted manuscript posted online 20 July 2016

Citation Li D, Chen T, Hu Y, Zhou Y, Liu Q, Zhou D, Jin X, Huang Z. 2016. An Ebola virus-like particle-based reporter system enables evaluation of antiviral drugs *in vivo* under non-biosafety level 4 conditions. J Virol 90:8720–8728. doi:10.1128/JVI.01239-16.

Editor: D. S. Lyles, Wake Forest University

Address correspondence to Zhong Huang, huangzhong@ips.ac.cn.

D.L. and T.C. contributed equally to this work.

measuring β-lactamase activity (18). However, the fusion of β-lactamase to VP40 slightly impaired the assembly of virus-like particles (VLPs) (18). Recently, another model was developed for studying the EBOV life cycle, based on replication- and transcription-competent VLPs containing tetracistronic minigenomes (19). Although complex, the system allows *in vitro* modeling of the EBOV life cycle over several infectious cycles under BSL-2 conditions. The above-described *in vitro* systems have significantly advanced the tools for EBOV research. However, there is no *in vivo* infection model available outside BSL-4 facilities at present.

Based on the observation that EBOVLP can package actin into the particles during budding (20, 21) and that it is capable of packaging reporter proteins, such as luciferase (22), we hypothesized that a reporter-containing EBOVLP could be generated and used to deliver reporter proteins into animals, thereby creating a non-BSL-4 *in vivo* model of EBOV entry. To test this hypothesis, we constructed an EBOVLP coupled with a Fluc reporter and have demonstrated that the reporter EBOVLP could be easily produced and safely used. Notably, the novel reporter EBOVLP not only morphologically resembles the authentic EBOV, but also functionally mimics EBOV in its entry into target cells and thus is most suited for the identification of anti-EBOV drugs and neutralizing antibodies targeting the entry step both *in vitro* and *in vivo*.

MATERIALS AND METHODS

Cell lines and antibodies. HEK293T cells and Vero cells were purchased from the Chinese Academy of Sciences Cell Bank of Type Culture Collection (CBTCCCAS) (Shanghai, China) and maintained in complete Dulbecco's modified Eagle's medium (DMEM) (Gibco) supplemented with 10% fetal bovine serum (FBS) (Gibco) and 1% penicillin-streptomycin (Gibco).

EBOV NP-specific monoclonal antibody (MAb) was kindly provided by Zhiyong Ma (Shanghai Veterinary Research Institute, Chinese Academy of Agricultural Science). EBOV VP40-specific polyclonal antibody was generated in house from mice immunized with *Escherichia coli*-expressed VP40 protein. Two EBOV GP-specific MAbs, 13C6 and 6D8 (23), were produced in HEK293T cells by cotransfection with plasmids encoding the heavy and light chains of the corresponding antibody and subsequently purified using a HiTrap rProtein A FF column (GE Healthcare). The firefly luciferase-specific antibody was purchased from Abcam (catalog no. ab185924). Niemann-Pick C1 (NPC1) antibody was purchased from Abcam (catalog no. ab134113). Fluorescein isothiocyanate (FITC)-conjugated early endosomal antigen 1 (EEA1) antibody (BD; catalog no. 612006) and Cy3-conjugated lysosomal-associated membrane protein 1 (LAMP-1) antibody (Abcam; catalog no. ab67283) were used to label early endosomes and late endosomes in the immunofluorescence assay.

Plasmid construction. Genes encoding GP, VP40, and NP of EBOV (Ebola virus H.sapiens-wt/GIN/2014/Makona-Gueckedou-C07; GenBank accession no. KJ660347) were codon optimized and synthesized by GenScript (Nanjing, China). The synthesized genes were cloned into the backbone vector pcDNA3.1, yielding plasmids pcDNA-EBOV-GP, pcDNA-EBOV-VP40, and pcDNA-EBOV-NP, respectively. The accuracy of the above-mentioned constructs was verified by sequencing.

EBOVLP expression and purification. To produce Fluc-packaged EBOVLP (designated EBOVLP/Fluc/GP$^+$), HEK293T cells were cotransfected with pcDNA-EBOV-GP, pcDNA-EBOV-VP40, and pcDNA-EBOV-NP, as well as pLenti6-Fluc (24), using polyethylenimine (PEI) (Sigma; catalog no. 408727). The cell medium was replaced with complete DMEM containing 10 μM sodium butyrate at 4 h posttransfection and then refreshed with FS293 medium 12 h later. Supernatants were collected after 48 h and clarified by centrifugation. EBOVLP without envelope protein GP (designated EBOVLP/Fluc/GP$^-$) was also generated by cotransfecting HEK293T cells with pcDNA-EBOV-VP40, pcDNA-EBOV-NP, and pLenti6-Fluc. For VLP purification, supernatants containing EBOVLP were layered onto 25% sucrose cushions and subjected to ultracentrifugation at 27,000 rpm for 3 h. The resultant pellets were resuspended in phosphate-buffered saline (PBS) and then layered onto 20 to 60% sucrose gradients for ultracentrifugation at 39,000 rpm for 2 h. Fractions were harvested and analyzed by enzyme-linked immunosorbent assay (ELISA), and Western blot and luciferase assays were performed as described below. Then, EBOV protein-rich fractions were pooled and sedimented through a 25% sucrose cushion. The resulting pellet was resuspended in PBS, giving rise to purified EBOVLP preparations. Purified EBOVLP was quantified for VP40 content by Western blotting with *E. coli*-expressed VP40 protein as the reference standard and anti-VP40 as the detection antibody.

EBOVLP transduction *in vitro*. For *in vitro* transduction experiments, purified EBOVLP (equivalent to 150 ng of VP40 per well) was added to preseeded Vero cells (1×10^4/well) on 96-well plates. The inoculated cells were incubated at 4°C or 37°C for different periods, as indicated. Then, the cells were harvested, washed with PBS 3 or 4 times, and lysed with 50 μl of cell lysis reagent (Promega). The resulting lysates were subjected to luciferase assay. Briefly, 30 μl of luciferase substrate (Promega) was added to each sample, and luciferase activity was determined in a Varioskan flash multimode reader.

EBOV GP-pseudotyped lentivirus infection assay. EBOV GP-pseudotyped HIV (HIV/EBOVpv) was generated as previously described (13). Briefly, HEK293T cells were cotransfected with the HIV packaging plasmid psPAX2 (25), pLenti6-Fluc, and pcDNA-EBOV GP using PEI. Supernatants were collected after 48 h and clarified by centrifugation. For infection assays, HIV/EBOVpv supernatants were first normalized according to their HIV p24 levels by ELISA and then used to infect cells preseeded (1×10^4 cells/well) in 96-well plates. Luciferase assays were performed as described above at 72 h postinfection.

Quantitative PCR. To detect the existence of Fluc plasmid in the sucrose gradient fractions, total DNA was extracted from each fraction using a Tianamp Genomic DNA kit and then used for determination of the Fluc gene copy number by a quantitative PCR (qPCR) assay with a pair of primers (forward, 5′-CTCGGATCCACCGCCATGGAAGACGCCAAAAACATAAAG-3′; reverse, 5′-CCCTCTAGATTACACGGCGATCTTTCCGCCCTTC-3′).

SDS-PAGE and Western blotting. SDS-PAGE and Western blot assays were performed according to standard procedures. The blots were probed with protein-specific primary antibodies as indicated, followed by incubation with the corresponding horseradish peroxidase (HRP)- or alkaline phosphatase (AP)-conjugated secondary antibodies.

ELISA. Protein samples diluted to appropriate concentrations in PBS were added to wells of 96-well ELISA plates, followed by incubation at 4°C overnight. The wells were blocked with 5% nonfat milk for 1 h, and the samples were incubated with 50 μl (5 μg/ml) of 13C6 MAb for 2 h, followed by incubation with goat anti-human IgG-HRP (Sigma) for 1 h. After each incubation step, the plates were washed three times with PBST (PBS plus 0.05% Tween 20). After color development, absorbance was measured at 450 nm using a 96-well plate reader.

Electron microscopy. Purified EBOVLP samples were adsorbed onto carbon-coated copper grids, negatively stained with 0.2% phosphotungstic acid, and examined under a 120-kV transmission electron microscope (Tecnai Spirit TEM; FEI).

Immunofluorescence assay. For immunofluorescence assays, 1×10^5 Vero cells were seeded on glass coverslips placed in wells of 24-well plates and subsequently incubated at 37°C for 12 h. The cells were cooled at 4°C for 15 min and then inoculated with purified EBOVLP/Fluc/GP$^+$ or EBOVLP/Fluc/GP$^-$, followed by incubation at 37°C. The cells were fixed with fixation buffer (4% paraformaldehyde in PBS) at the indicated time points. The fixed cells were blocked for 1 h with blocking buffer (3% bovine serum albumin [BSA], 0.05% saponin, and 10% FBS in PBS), followed by incubation for 1 h with the indicated primary antibodies in binding buffer (1% BSA, 0.05% saponin, and 1% FBS in PBS). Corre-

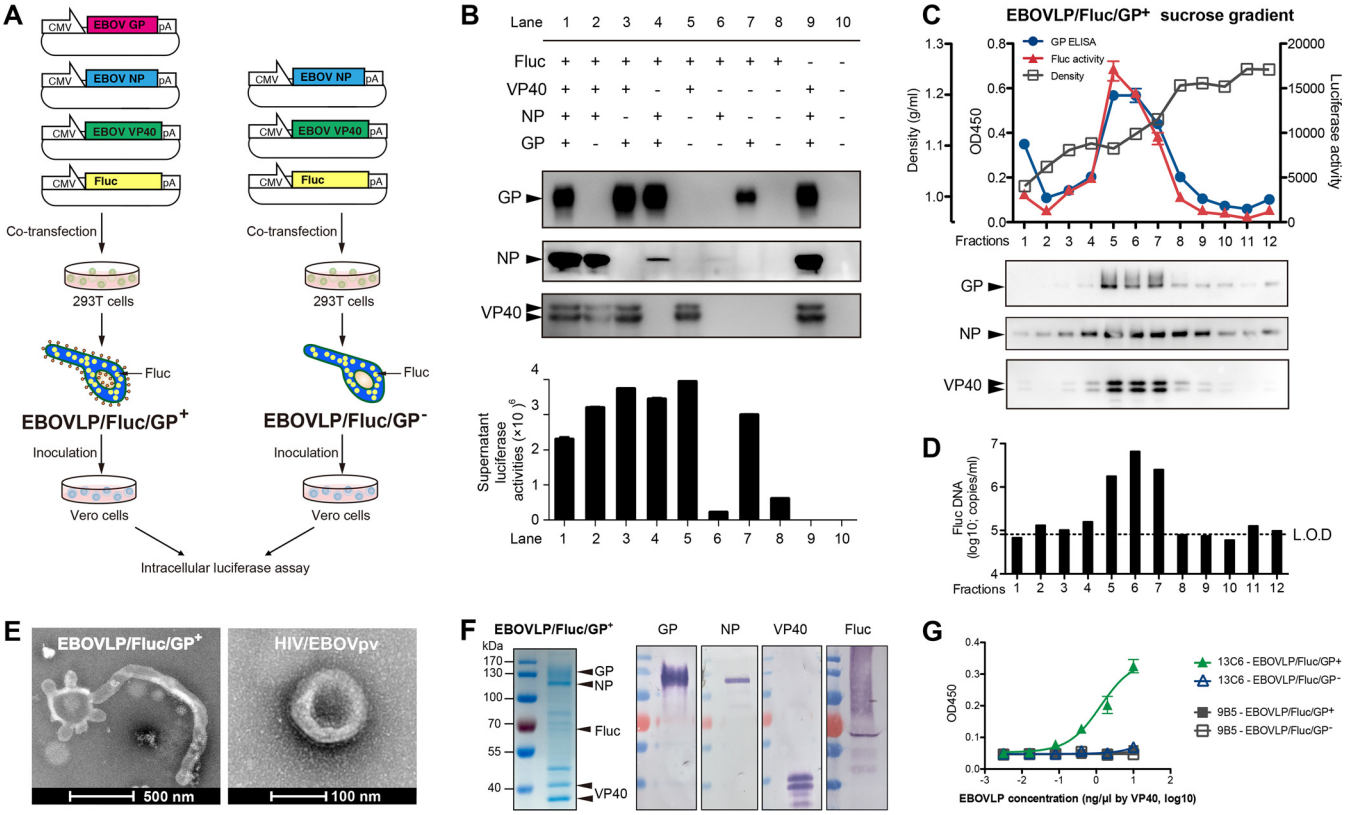

FIG 1 Construction and characterization of the reporter EBOVLP. (A) Schematic diagram of the generation of complete EBOVLP/Fluc/GP$^+$ and envelope-lacking EBOVLP/Fluc/GP$^-$. (B) Expression of GP, NP, VP40, and Fluc in the supernatant of HEK293T cells transfected with plasmids in different combinations. EBOV proteins GP, NP, and VP40 were identified by Western blotting, while the presence of Fluc was detected by luciferase assay. (C and D) Sucrose gradient analysis of cell culture supernatant containing EBOVLP/Fluc/GP$^+$. The presence of EBOV proteins in the collected fractions was detected by ELISA and Western blotting (C), while the distribution of Fluc protein and Fluc plasmid was tested by luciferase assay (C) and qPCR (D). The dashed line indicates the limit of detection (L.O.D). (E) Electron microscopy of purified EBOVLP/Fluc/GP$^+$ and HIV/EBOVpv. (F) SDS-PAGE and Western blot analyses of purified EBOVLP/Fluc/GP$^+$. The band(s) of each protein was verified by Western blotting using corresponding primary antibodies and alkaline phosphatase-conjugated secondary antibodies. (G) Recognition of EBOVLP/Fluc/GP$^+$ by an EBOV-neutralizing MAb, 13C6, but not a control MAb, 9B5, in ELISA. Means ± standard errors of the mean (SEM) of the optical density at 45 nm (OD_{450}) readings are shown.

sponding secondary antibodies were then added to the coverslips and incubated for 30 min. After brief washing, the coverslips were mounted with ProLong Gold Antifade Reagent (Molecular Probes) and examined under an Olympus FV1200 biological laser scanning microscope.

Mouse challenge and *in vivo* bioluminescence imaging. Female BALB/c mice (6 to 8 weeks old) were inoculated with EBOVLP/Fluc/GP$^+$ or EBOVLP/Fluc/GP$^-$ containing 2 μg of VP40 via tail vein injection. At the indicated time points postinoculation, mice were anesthetized using isoflurane inhalation anesthesia and injected intraperitoneally (i.p.) with 1.5 mg of VivoGlo Luciferin (Promega). Bioluminescence was measured, and three-dimensional (3D) optical tomographic reconstruction was performed using the IVIS SpectrumCT System (PerkinElmer). In the antibody protection experiment, EBOVLP/Fluc/GP$^+$ or EBOVLP/Fluc/GP$^-$ was mixed with the MAbs and incubated at room temperature for 1 h, and then the mixture was administered to BALB/c mice via tail vein injection. At 12 h postinoculation, an *in vivo* imaging assay was performed as described above. All animal studies were approved by the Institutional Animal Care and Use Committee at the Institut Pasteur of Shanghai.

Statistics analysis. For significance comparisons, nonparametric one-way analysis of variance (ANOVA) with Bonferroni's correction or Student's *t* test was used. Significance at *P* values of ≥0.05 were considered not significant, *P* values of <0.05 were considered significant, *P* values of <0.01 were considered highly significant, and *P* values of <0.001 were considered extremely significant. All statistical analyses were performed with GraphPad Prism 5.0c (GraphPad Software, La Jolla, CA).

RESULTS

Expression and characterization of Fluc-incorporating EBOVLP. To generate EBOVLP packaging Fluc proteins, we adopted a strategy similar to that used to produce reporter lentiviruses (Fig. 1A) (13). Plasmids encoding Fluc, VP40, NP, or GP were cotransfected in different combinations into HEK293T cells (Fig. 1B), and the supernatant from transfected cell cultures was analyzed for protein expression and VLP assembly. As shown in Fig. 1B, the EBOV proteins were expressed as expected for the corresponding plasmid combinations. We also analyzed the supernatant by luciferase assay. High luciferase activity was detected in the samples cotransfected with the Fluc plasmid and the VP40 plasmid (Fig. 1B, lanes 1, 2, 3, and 5), but not in the sample transfected with the Fluc plasmid alone (lane 8). Because it was reported previously that sole expression of VP40 (26) or coexpression of VP40, NP, and GP led to VLP assembly (27, 28), the luciferase data presented here strongly suggest that Fluc was packaged into the VP40 VLPs. The sample cotransfected with the Fluc and NP plasmids (Fig. 1B, lane 6) did not show detectable luciferase activity, suggesting the absence of Fluc-incorporated VLPs, which is consistent with a previous finding that NP alone does not assemble VLPs (29). Interestingly, significant luciferase activity was also detected in the

medium of cells expressing NP plus GP (Fig. 1B, lane 4) or GP (lane 7). Because GP alone cannot form VLP (15), the presence of Fluc in these samples may be a reflection of the known cytotoxicity mediated by GP (30), which permeates the cell membrane and consequently results in the release of the Fluc protein into the supernatant. As NP and GP enhance the production of VP40 VLPs in concert (27, 28), our subsequent analyses were focused on the samples transfected with the VP40-NP-GP-Fluc plasmid combination.

To evaluate VLP assembly, the supernatant of HEK293T cells cotransfected with the VP40-NP-GP-Fluc plasmids was subjected to sucrose gradient ultracentrifugation. Analysis of the resulting gradient fractions by ELISA and Western blot and luciferase assays revealed cosedimentation of GP, NP, VP40, and Fluc with a profile typical for particulate structures (Fig. 1C). These data provide strong evidence that GP, NP, VP40, and Fluc may have coassembled into VLPs. The Fluc DNA was also detected in peak fractions containing GP-NP-VP40-Fluc (Fig. 1D). Therefore, it is possible that the Fluc plasmid was also packaged in the VLPs.

The VP40-NP-GP-Fluc-rich gradient fractions were subjected to ultracentrifugation, and the resulting putative VLP preparations were examined by electron microscopy. As shown in Fig. 1E, filamentous structures with diameters of ~100 nm and lengths of over 1 μm, which is the typical morphology of the authentic EBOV and other EBOVLP reported previously (15, 16, 31, 32), were evident. In contrast, HIV/EBOVpv were smaller, spherical particles with a diameter of ~100 nm (Fig. 1E). Collectively, the above-mentioned results demonstrate that coexpression of GP-NP-VP40-Fluc resulted in the assembly of Fluc-incorporating EBOVLP (denoted EBOVLP/Fluc/GP$^+$ here).

For further characterization, highly purified EBOVLP/Fluc/GP$^+$ was obtained and subjected to biochemical analyses. The results of SDS-PAGE and Western blot assay showed that EBOVLP/Fluc/GP$^+$ indeed consisted of GP, NP, VP40, and Fluc (Fig. 1F). EBOVLP/Fluc/GP$^+$ was then tested in ELISA for binding to a GP-specific neutralizing monoclonal antibody, 13C6, which recognizes a conformational epitope (8). As shown in Fig. 1G, EBOVLP/Fluc/GP$^+$ reacted with 13C6, but not with the irrelevant control antibody 9B5, in a dose-dependent manner, suggesting that the conformation of GP on the VLP resembles that on the authentic virus.

EBOVLP/Fluc/GP$^+$ is capable of delivery of luciferase into target cells. To explore the utility of EBOVLP/Fluc/GP$^+$ as a reporter in EBOV research, we first investigated whether EBOVLP/Fluc/GP$^+$ could deliver Fluc into target cells. We inoculated EBOVLP/Fluc/GP$^+$ onto Vero cells and then evaluated the intracellular luciferase activity at different time points. EBOVLP lacking GP (designated EBOVLP/Fluc/GP$^-$), which was produced from cells cotransfected with the VP40, NP, and Fluc plasmids, was used as a negative control in the assay. The results showed that significant luciferase activity was detected in the EBOVLP/Fluc/GP$^+$-inoculated samples, but not in those treated with EBOVLP/Fluc/GP$^-$ (Fig. 2A). The Fluc signals peaked at 6 h postinoculation and dropped gradually for the next 3 days but remained detectable even at 72 h postinoculation (Fig. 2A). These data suggest that EBOVLP-mediated Fluc delivery depends on the presence of GP.

To verify whether EBOVLP/Fluc/GP$^+$ can be efficiently taken up, EBOVLP/Fluc/GP$^+$-attached cells were incubated at 37°C for different periods before being treated with trypsin to remove VLPs bound on the cell surface. Cells with and without trypsin treatment were assayed in parallel for luciferase activity. As shown in Fig. 2B, trypsin treatment prior to 37°C incubation (0 min) almost completely abolished luciferase activity, and early administration (5 min) of trypsin resulted in substantially decreased Fluc signal, whereas no significant difference in luciferase activity was observed between the trypsin-treated and untreated samples when the cells had been incubated at 37°C for 15 min or longer. The above-mentioned results suggest that EBOVLP/Fluc/GP$^+$ internalization is an efficient process and may be completed within 15 min postattachment.

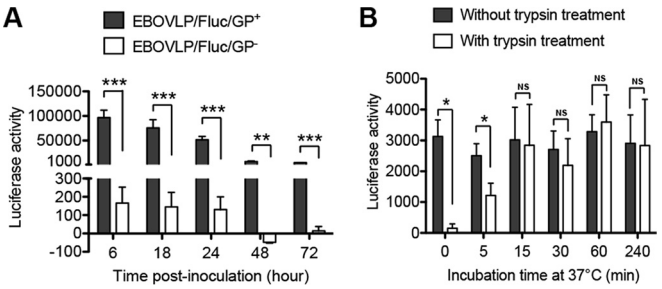

FIG 2 EBOVLP/Fluc/GP$^+$ is capable of delivery of luciferase into target cells. (A) Kinetics of luciferase activities in target cells inoculated with either EBOVLP/Fluc/GP$^+$ or EBOVLP/Fluc/GP$^-$. GP-bearing EBOVLP/Fluc/GP$^+$, as well as GP-lacking EBOVLP/Fluc/GP$^-$, generated from the transfected HEK293T cell cultures was inoculated onto fresh Vero cells. Vero cell samples were harvested at the indicated time points, washed, and then assayed for luciferase activity. (B) Trypsin treatment experiment. Vero cells were incubated with EBOVLP/Fluc/GP$^+$ at 4°C for 1 h to allow attachment, followed by washing out the unattached VLPs and transferring to 37°C. At the indicated time points, cell samples were harvested, washed, and treated with trypsin (final concentration, 2.5 mg/ml) for 3 min to remove the VLPs on the surface. Cells without trypsin treatment were set as controls. All the samples were then subjected to luciferase assay. Mean values ± SEM are shown. The asterisks represent significant differences: NS, no significance ($P \geq 0.05$); *, $P < 0.05$; **, $P < 0.01$; ***, $P < 0.001$.

Previous studies showed that EBOV enters host cells via endocytosis and macropinocytosis (33–35). To visualize the association of our reporter EBOVLP with endosomes, cells inoculated with EBOVLP/Fluc/GP$^+$ or EBOVLP/Fluc/GP$^-$ were subjected to immunofluorescence assay and confocal microscopy. EBOVLP/Fluc/GP$^-$-inoculated cells were free of VP40 signal regardless of the incubation time at 37°C (Fig. 3), suggesting that EBOVLP/Fluc/GP$^-$ cannot efficiently bind to cells due to the lack of GP. In the EBOVLP/Fluc/GP$^+$-inoculated cells, VP40 was first detected at the cell periphery and then observed entering intracellular regions from 5 min to 30 min with increasing colocalization with EEA1, an early endosome marker (Fig. 3A). However, at the 120-min time point, VP40 was found significantly colocalized with LAMP1 (Fig. 3B), a late endosome/lysosome marker, but not with EEA1 (Fig. 3A), suggesting EBOVLP/Fluc/GP$^+$ trafficking from early endosomes to late endosomes.

We further performed the double-staining assay with anti-VP40 and an antibody against NPC1, a key receptor of EBOV (36). In the EBOVLP/Fluc/GP$^+$-inoculated cells, VP40 appeared to move from the cell periphery to intracellular regions, with a certain rate of colocalization with NPC1 detected at the 120-min time point (Fig. 3C), suggesting EBOVLP/Fluc/GP$^+$ was associated with NPC1 at a late entry step. In contrast, VP40 was not detected in the EBOVLP/Fluc/GP$^-$-inoculated cells (Fig. 3A to C). These results are consistent with a previous finding that GP-bearing

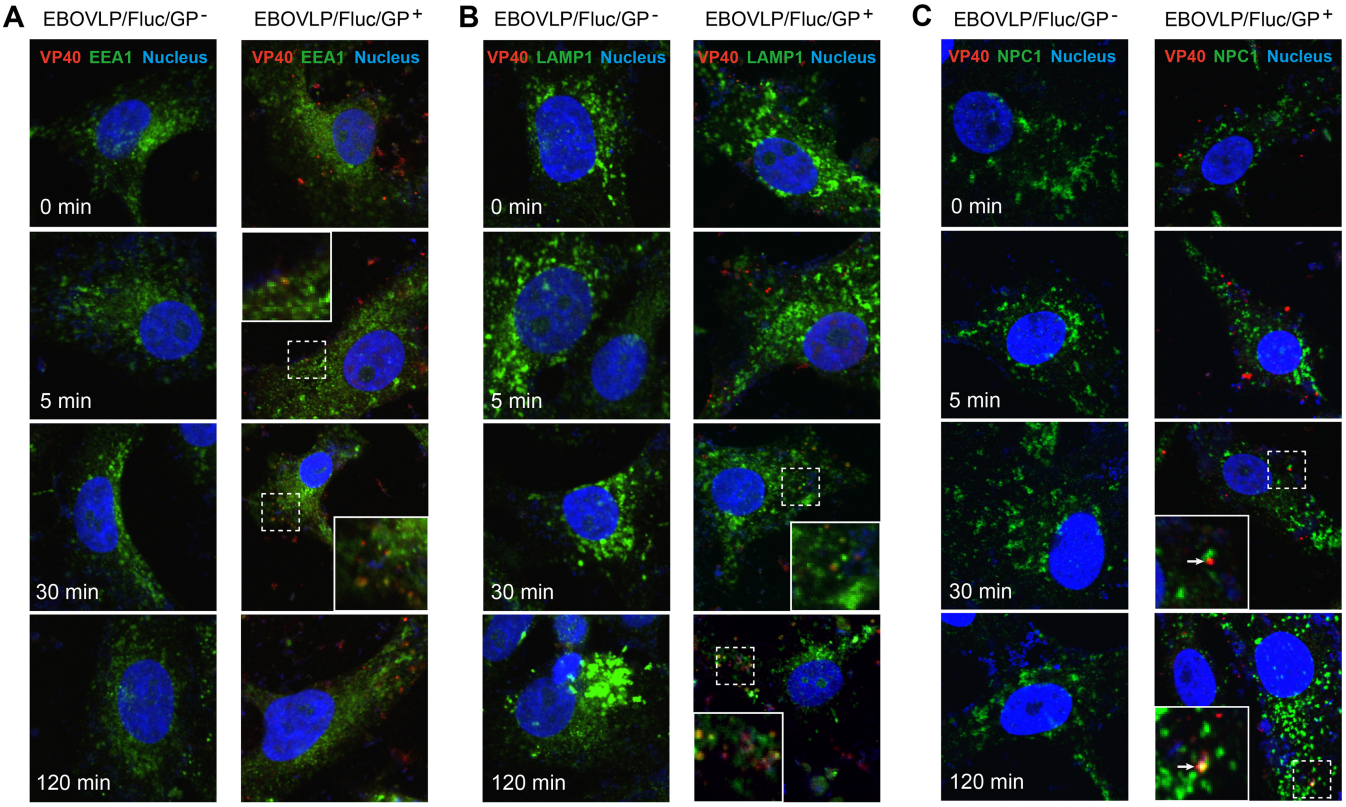

FIG 3 Immunofluorescence assays. Vero cells were preattached by EBOVLP/Fluc/GP$^+$ or EBOVLP/Fluc/GP$^-$ at 4°C for 1 h and then incubated at 37°C for the indicated times before double staining of VP40 and EEA1 (A), VP40 and LAMP1 (B), and VP40 and NPC1 (C). The cells were also stained with Hoechst to show nuclei. The images were captured by confocal microscopy and adjusted to pseudocolors. (A) Red, VP40; green, EEA1; blue, Hoechst. (B) Red, VP40; green, LAMP1; blue, Hoechst. (C) Red, VP40; green, NPC1; blue, Hoechst. Areas of overlap are shown in yellow. Representative micrographs for the 0-min, 5-min, 30-min, and 120-min time points are shown. The insets are enlarged views of the areas outlined with dashed lines.

EBOVLP enters the cytoplasm through NPC1$^+$ endosomes/lysosomes (34).

EBOVLP/Fluc/GP$^+$ delivery is sensitive to neutralizing antibody in the cell culture model. To explore the potential utility of EBOVLP/Fluc/GP$^+$ in high-throughput drug screening, we examined whether the entry of EBOVLP/Fluc/GP$^+$ into permissive cells can be blocked by neutralizing antibodies. A known anti-EBOV neutralizing monoclonal antibody, 13C6 (8, 23), was used as the model antibody in the experiment. As shown in Fig. 4A, 13C6 neutralized EBOVLP/Fluc/GP$^+$ entry in a dose-dependent manner, whereas an irrelevant control MAb, 9B5, exhibited no neutralization. Similar trends of antibody dose-dependent neutralization (Fig. 4B) were also observed when the antibodies were evaluated using EBOV GP-pseudotyped HIV (denoted HIV/EBOVpv) (17, 18). Our results are overall consistent with the antibodies' neutralization activities determined using infectious EBOV (7), thus validating the use of EBOVLP/Fluc/GP$^+$ in the screening and evaluation of neutralizing antibodies.

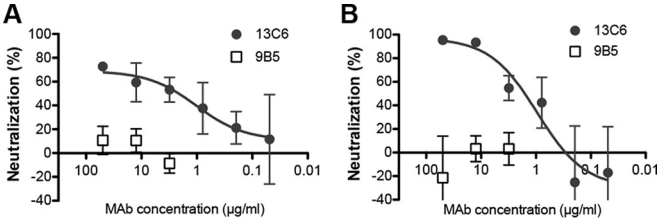

FIG 4 EBOVLP/Fluc/GP$^+$ entry is sensitive to neutralizing antibody in the cell culture model. Anti-EBOV MAb 13C6 was diluted to the indicated concentrations and mixed with EBOVLP/Fluc/GP$^+$ (A) or HIV/EBOVpv (B), followed by incubation at 37°C for 1 to 2 h. Then, the mixtures were added to Vero cells, followed by incubation at 37°C. Six hours later, the culture medium was replaced with fresh medium. At 72 h postinoculation, the cells were analyzed by luciferase assay. An irrelevant MAb, 9B5, was used as a negative control in the experiment. The error bars indicate SEM.

EBOVLP/Fluc/GP$^+$ is capable of entering cells *in vivo*. We further investigated whether EBOVLP/Fluc/GP$^+$ could deliver luciferase into mouse cells *in vivo*. First, we compared the entry abilities of EBOVLP/Fluc/GP$^+$ and EBOVLP/Fluc/GP$^-$ in mouse cell lines and primary cells isolated from organs and discovered that EBOVLP/Fluc/GP$^+$ has broad tropism and is capable of transducing all three mouse cell lines (Hepa1-6, NIH 3T3, and L929) with different tissue origins (liver, fibroblast, and connective tissue) and establishing a presence in primary cells isolated from various organs postinoculation (Fig. 5A and B). In contrast, EBOVLP/Fluc/GP$^-$ inoculation did not yield significant signal in the same target cells (Fig. 5A and B). Next, we investigated the *in vivo* transducing activity of EBOVLP/Fluc/GP$^+$ in mice. BALB/c mice were inoculated with EBOVLP/Fluc/GP$^+$ or EBOVLP/Fluc/GP$^-$ by tail vein injection and subsequently monitored for bioluminescent signals by *in vivo* live imaging. Consistent with the *in*

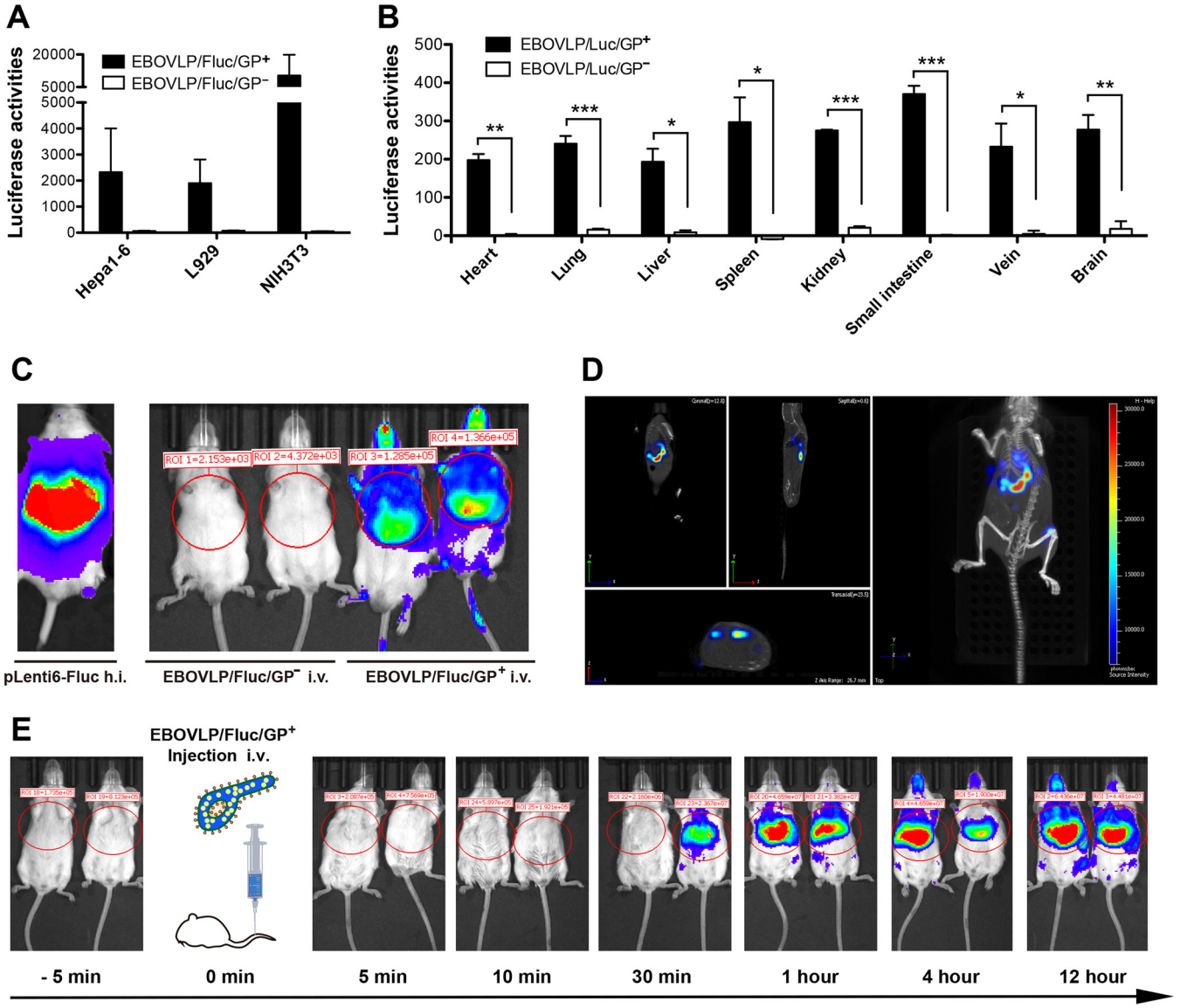

FIG 5 EBOVLP/Fluc/GP$^+$ inoculation produces bioluminescence in mice. (A) EBOVLP/Fluc/GP$^+$ delivery in different mouse cell lines, including Hepa1-6, L929, and NIH 3T3. (B) *Ex vivo* tropism of EBOVLP/Fluc/GP$^+$. Mouse cells isolated from main organs (heart, lung, liver, spleen, kidney, small intestine, vena cava, and brain) of BALB/c mice were inoculated with EBOVLP/Fluc/GP$^+$ and subsequently analyzed for intracellular luciferase activity. Mean values plus SEM are shown. The asterisks represent significant differences: *, $P < 0.05$; **, $P < 0.01$; ***, $P < 0.001$. (C) EBOVLP/Fluc/GP$^+$ challenge of BALB/c mice. Six-week-old BALB/c mice were challenged by intravenous (i.v.) injection with VP40-normalized (2 μg) EBOVLP/Fluc/GP$^+$ or EBOVLP/Fluc/GP$^-$. PBS was given as a negative control, while hydrodynamic injection (h.i.) of the pLenti6-Fluc plasmid (100 μg/mouse) was set as a positive control. *In vivo* imaging was performed 12 h postinoculation. (D) Representative 3D bioluminescence from EBOVLP/Fluc/GP$^+$-inoculated mice. 3D imaging was performed at 12 h postinoculation using the IVIS SpectrumCT system. (E) Dynamics of bioluminescence in EBOVLP/Fluc/GP$^+$-inoculated mice. The inoculated mice were subjected to live imaging at the indicated time points. The images were adjusted and are shown at the same scale.

vitro results, the mice that had been inoculated with EBOVLP/Fluc/GP$^+$ produced striking bioluminescence throughout the body, whereas no significant signal was observed in the control mice (inoculated with EBOVLP/Fluc/GP$^-$) (Fig. 5C). Further 3D optical tomographic reconstruction revealed that the primary target organ of EBOVLP/Fluc/GP$^+$ was the liver, where bioluminescent signal was intense in both the left and right lobes (Fig. 5D). These data demonstrate the successful establishment of an EBOVLP/Fluc/GP$^+$-based *in vivo* challenge model.

We then determined the dynamics of EBOVLP/Fluc/GP$^+$ entry *in vivo*. After EBOVLP/Fluc/GP$^+$ inoculation, mice were monitored for bioluminescence over a 12-h period. Bioluminescence was not detected until 30 min postinfection, and Fluc signals gradually increased from 30 min to 1 h postinfection and remained stable thereafter (Fig. 5E).

Anti-EBOV neutralizing antibody blocks EBOVLP/Fluc/GP$^+$ entry in mice. To test whether bioluminescent imaging of EBOVLP/Fluc/GP$^+$-challenged mice could be used as a readout to evaluate the efficacy of neutralizing antibodies or antiviral compounds, we performed proof-of-concept studies with the known EBOV-protective MAb 13C6 (23). First, we tested whether preincubation of the MAb and EBOVLP/Fluc/GP$^+$ before inoculation

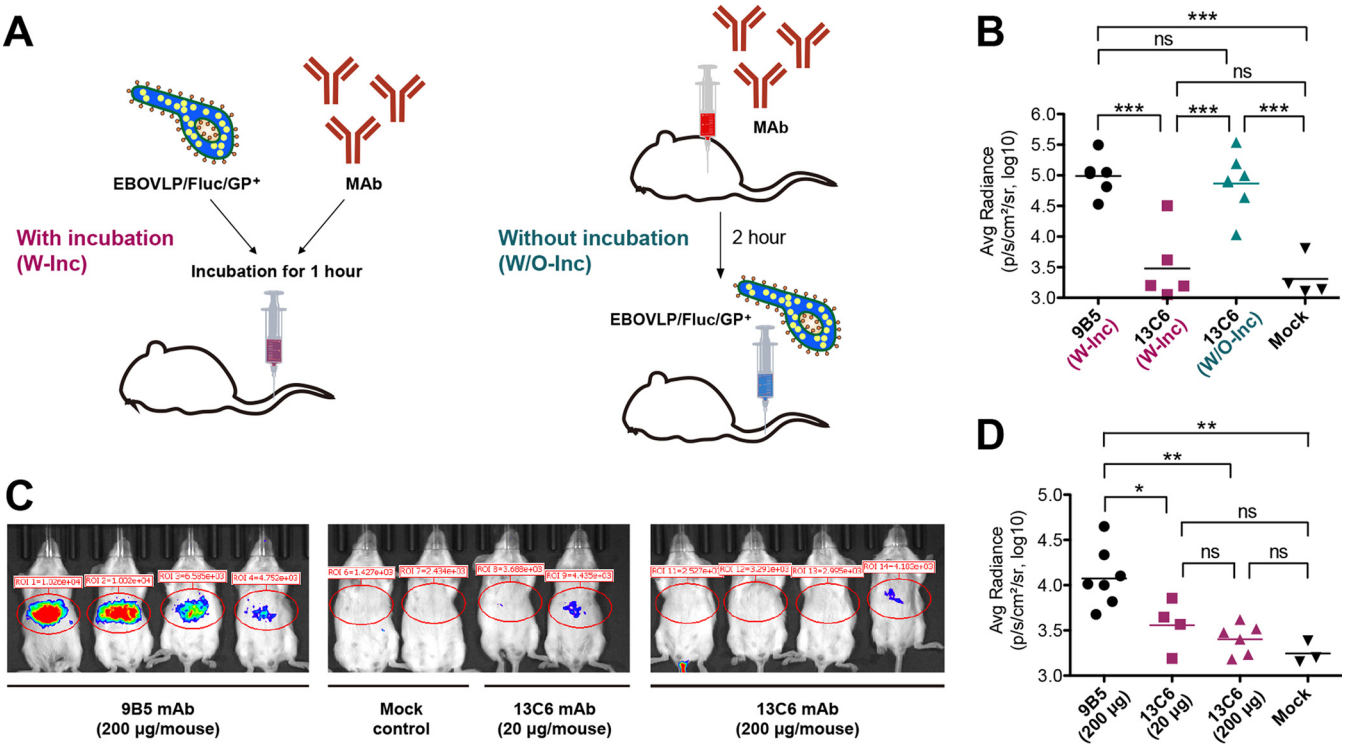

FIG 6 Anti-EBOV neutralizing antibody 13C6 blocks EBOVLP/Fluc/GP$^+$ entry in mice. (A) Schematic diagram of the two administration methods in mice. In the "with incubation" method, VP40-normalized EBOVLP/Fluc/GP$^+$ was mixed with MAb. After incubation, the mixtures were administered i.v. to BALB/c mice. In the "without incubation" method, MAb was given i.p. 2 h before EBOVLP/Fluc/GP$^+$ inoculation. (B) *In vivo* inhibitory effects of 13C6 MAb administered using the two methods shown in panel A. An irrelevant MAb, 9B5, served as the antibody control. (C) MAb 13C6 blocks EBOVLP/Fluc/GP$^+$ entry in mice. The indicated doses of 13C6 and the control MAb were evaluated by using the W-Inc method. *In vivo* bioluminescence imaging was performed at 12 h postinoculation. Representative images are shown. (D) Measurement of bioluminescence in mice from different treatment groups. Data from two independent experiments are shown. (B and D) The horizontal lines indicate the geometric means of each animal group. The significance of differences between groups was analyzed by nonparametric one-way ANOVA with Bonferroni's correction and shown as follows: ns, no significance ($P \geq 0.05$); *, $P < 0.05$; **, $P < 0.01$; ***, $P < 0.001$.

is required for *in vivo* inhibition (Fig. 6A). As shown in Fig. 6B, preincubation of EBOVLP/Fluc/GP$^+$ with 13C6 resulted in significantly less bioluminescence than the control (preincubation with the irrelevant antibody 9B5), whereas inoculation of EBOVLP/Fluc/GP$^+$ into 13C6-pretreated mice produced bioluminescent signal at levels similar to that of the control group, thus indicating the necessity for the preincubation procedure in this model. Consequently, we performed the protection experiment following the first method (with antibody preincubation), as indicated in Fig. 6A. As shown in Fig. 6C, in the presence of 20 μg or 200 μg of 13C6, Fluc delivery by EBOVLP/Fluc/GP$^+$ was significantly inhibited, as manifested by reduction of the bioluminescent signal (Fig. 6C, middle) to a level comparable to that of controls, whereas the irrelevant control MAb (9B5) did not decrease bioluminescent signals (Fig. 6C, left). The average bioluminescence intensity for individual animals tested is shown in Fig. 6D. These results thus demonstrate the *in vivo* use of the EBOVLP/Fluc/GP$^+$ model for testing the protective efficacy of anti-EBOV compounds under non-BSL-4 conditions.

DISCUSSION

The primary aim of the present study was to develop a noninfectious animal model for *in vivo* evaluation of anti-EBOV drug candidates. Our work demonstrates that the EBOVLP/Fluc/GP$^+$-based system is suitable for high-throughput screening of neutralizing antibodies against EBOV, both *in vitro* and *in vivo*.

Coexpression of VP40, GP, NP, and Fluc in HEK293T cells resulted in the production of EBOVLP/Fluc/GP$^+$, in which Fluc protein was packaged. Similar to live EBOV and nonreporter EBOVLP (34, 35, 37), EBOVLP/Fluc/GP$^+$ could bind efficiently to the cell surface and could be internalized rapidly (starting at approximately 5 min postattachment) (Fig. 2 and 3). Notably, EBOVLP/Fluc/GP$^+$ was able to deliver Fluc protein into target cells *in vitro* (Fig. 2) and therefore can be used as a reporter system for *in vitro* antiviral evaluation. In this study, we demonstrated that the neutralizing MAb 13C6, which is one of the three components of the ZMapp antibody cocktail (7, 8), could inhibit EBOVLP/Fluc/GP$^+$ entry *in vitro* (Fig. 4), thus validating the application of EBOVLP/Fluc/GP$^+$ in screening entry inhibitors, such as neutralizing MAbs. Unlike other surrogate systems, such as EBOV GP-pseudotyped reporter viruses (10, 11), EBOVLP/Fluc/GP$^+$ resembles infectious EBOV in overall morphology and GP conformation (Fig. 1), which may be critical for faithful determination of the capacity of MAbs to neutralize authentic EBOVs. Indeed, a recent study showed that EBOV GP-pseudotyped VSV did not accurately predict the neutralization activities of MAbs against authentic EBOV (38). Therefore, EBOVLP/Fluc/GP$^+$ may represent a more suitable plat-

form for evaluating neutralizing MAbs than the currently available surrogate systems. Moreover, following our protocol, reporter VLPs incorporating GP from different strains of EBOV could be easily generated by swapping the GP construct, thus enabling the evaluation of cross-neutralization against heterologous strains.

In the present study, we found that EBOVLP/Fluc/GP$^+$ could enter mouse cells both *in vitro* and *in vivo*. Mice inoculated with EBOVLP/Fluc/GP$^+$ yielded bioluminescence that could be monitored by live imaging (Fig. 5). We further showed that pretreatment with the neutralizing MAb 13C6 could block the production of bioluminescent signals in EBOVLP/Fluc/GP$^+$-inoculated mice (Fig. 6). These results indicate that EBOVLP/Fluc/GP$^+$ can be used as a reporter system to investigate EBOV entry *in vivo* and to evaluate the protective efficacy of neutralizing antibodies or candidate vaccines. It is particular valuable as a rapid *in vivo* screening tool for Ebola vaccines and drugs to be tested more stringently in BSL-4 laboratories, thus providing great cost saving and significant improvement of efficiency.

Reconstruction of bioluminescence by 3D optical tomographic scanning identified the liver as the main organ/tissue location of EBOVLP/Fluc/GP$^+$ entry (Fig. 5D). This finding is consistent with the fact that the liver is a major target organ for EBOV, where the virus replicates to high titers and extensive necrosis occurs in mouse and nonhuman primate models of EBOV infection (reviewed in references 39 and 40) and in EBOV-infected human individuals (reviewed in reference 41). Specifically, it has been reported that, in mice inoculated i.p. with 100 PFU of mouse-adapted EBOV, a high virus titer (10^4 PFU/g) was detected in the liver 1 day after virus challenge, which then increased to approximately 10^7 PFU/g on day 2 postinoculation (42). The mechanism for the liver tropism observed in our mouse model remains unclear. It is possible that some liver-specific or liver-enriched molecules, such as the C-type lectin asialoglycoprotein receptor (43), the liver and/or lymph node-specific intercellular adhesion molecule 3-grabbing nonintegrin (L-SIGN) (44), the liver and lymph node sinusoidal endothelial cell C-type lectin (LSECTin) (45, 46), and highly sulfated heparan sulfate (47, 48), may have played a significant role in this phenomenon. These molecules might act as cellular attachment receptors in the liver, allowing local enrichment/concentration of EBOVLP/Fluc/GP$^+$. We should point out that EBOVLP/Fluc/GP$^+$-inoculated mice were not treated with trypsin, and therefore, the detected bioluminescence might be contributed by both cell surface-bound VLPs and those that have penetrated/crossed the plasma membrane. However, based on the *in vitro* finding that EBOVLP internalization from the cell surface occurred rapidly (5 to 15 min) following attachment (Fig. 2B) (34), we reason that the *in vivo* bioluminescence signals detected at time points beyond 1 h postinoculation should be mainly produced by VLPs that had been at least internalized. The half-life of soluble Fluc is usually 3 to 4 h (49). In the present study, we found that EBOVLP/Fluc/GP$^+$-inoculated mice produced strong bioluminescence even at 12 h postinoculation (Fig. 5E). Similarly, a high level of Fluc activity was detected in the EBOVLP/Fluc/GP$^+$-transduced cell cultures at 18 h postinoculation (Fig. 2A). These *in vitro* and *in vivo* data suggest that VLP-associated Fluc is somewhat protected from degradation, resulting in a prolonged half-life. The kinetics and fate of EBOVLP/Fluc/GP$^+$ remain to be further defined. Nonetheless, the application of the EBOVLP/Fluc/GP$^+$ system allows us to obtain a dynamic picture that may reflect the early phase of EBOV infection *in vivo*, thus representing a useful tool for EBOV research under non-BSL-4 conditions.

ACKNOWLEDGMENTS

We thank Zhiyong Ma (Shanghai Veterinary Research Institute, Chinese Academy of Agricultural Science) for providing the EBOV NP-specific MAb. We also thank Jin Zhong (Institut Pasteur of Shanghai) for providing the EBOV NP plasmid.

This study was supported in part by the Response-to-Ebola Program of the Institut Pasteur of Shanghai, Chinese Academy of Sciences (CAS) (KLMVI-Ebola-2014002).

FUNDING INFORMATION

This work, including the efforts of Zhong Huang, was funded by Chinese Academy of Sciences (CAS) (KLMVI-Ebola-2014002). This work, including the efforts of Dongming Zhou, Xia Jin, and Zhong Huang, was funded by Ministry of Science and Technology of the People's Republic of China (MOST) (2016YFC1201000).

The funders had no role in study design, data collection and interpretation, or the decision to submit the work for publication.

REFERENCES

1. **Baize S, Pannetier D, Oestereich L, Rieger T, Koivogui L, Magassouba N, Soropogui B, Sow MS, Keita S, De Clerck H, Tiffany A, Dominguez G, Loua M, Traore A, Kolie M, Malano ER, Heleze E, Bocquin A, Mely S, Raoul H, Caro V, Cadar D, Gabriel M, Pahlmann M, Tappe D, Schmidt-Chanasit J, Impouma B, Diallo AK, Formenty P, Van Herp M, Gunther S.** 2014. Emergence of Zaire Ebola virus disease in Guinea—preliminary report. N Engl J Med **371:**1418–1425. http://dx.doi.org/10.1056/NEJMoa1404505.
2. **WHO Ebola Response Team.** 2014. Ebola virus disease in West Africa—the first 9 months of the epidemic and forward projections. N Engl J Med **371:**1481–1495. http://dx.doi.org/10.1056/NEJMoa1411100.
3. **Cohen J, Enserink M.** 2015. Clinical trials. Ebola vaccines face daunting path to approval. Science **349:**1272–1273. http://dx.doi.org/10.1126/science.349.6254.1272.
4. **Kilgore PE, Grabenstein JD, Salim AM, Rybak M.** 2015. Treatment of Ebola virus disease. Pharmacotherapy **35:**43–53. http://dx.doi.org/10.1002/phar.1545.
5. **Muyembe-Tamfum JJ, Mulangu S, Masumu J, Kayembe JM, Kemp A, Paweska JT.** 2012. Ebola virus outbreaks in Africa: past and present. Onderstepoort J Vet Res **79:**451. http://dx.doi.org/10.4102/ojvr.v79i2.451.
6. **Warfield KL, Bosio CM, Welcher BC, Deal EM, Mohamadzadeh M, Schmaljohn A, Aman MJ, Bavari S.** 2003. Ebola virus-like particles protect from lethal Ebola virus infection. Proc Natl Acad Sci U S A **100:**15889–15894. http://dx.doi.org/10.1073/pnas.2237038100.
7. **Qiu X, Wong G, Audet J, Bello A, Fernando L, Alimonti JB, Fausther-Bovendo H, Wei H, Aviles J, Hiatt E, Johnson A, Morton J, Swope K, Bohorov O, Bohorova N, Goodman C, Kim D, Pauly MH, Velasco J, Pettitt J, Olinger GG, Whaley K, Xu B, Strong JE, Zeitlin L, Kobinger GP.** 2014. Reversion of advanced Ebola virus disease in nonhuman primates with ZMapp. Nature **514:**47–53. http://dx.doi.org/10.1038/nature13777.
8. **Wilson JA, Hevey M, Bakken R, Guest S, Bray M, Schmaljohn AL, Hart MK.** 2000. Epitopes involved in antibody-mediated protection from Ebola virus. Science **287:**1664–1666. http://dx.doi.org/10.1126/science.287.5458.1664.
9. **Ebihara H, Takada A, Kobasa D, Jones S, Neumann G, Theriault S, Bray M, Feldmann H, Kawaoka Y.** 2006. Molecular determinants of Ebola virus virulence in mice. PLoS Pathog **2:**e73. http://dx.doi.org/10.1371/journal.ppat.0020073.
10. **Towner JS, Paragas J, Dover JE, Gupta M, Goldsmith CS, Huggins JW, Nichol ST.** 2005. Generation of eGFP expressing recombinant Zaire ebolavirus for analysis of early pathogenesis events and high-throughput antiviral drug screening. Virology **332:**20–27. http://dx.doi.org/10.1016/j.virol.2004.10.048.
11. **Hoenen T, Groseth A, Callison J, Takada A, Feldmann H.** 2013. A

novel Ebola virus expressing luciferase allows for rapid and quantitative testing of antivirals. Antiviral Res **99:**207–213. http://dx.doi.org/10.1016/j.antiviral.2013.05.017.
12. **Johnson E, Jaax N, White J, Jahrling P.** 1995. Lethal experimental infections of rhesus monkeys by aerosolized Ebola virus. Int J Exp Pathol **76:**227–236.
13. **Wool-Lewis RJ, Bates P.** 1998. Characterization of Ebola virus entry by using pseudotyped viruses: identification of receptor-deficient cell lines. J Virol **72:**3155–3160.
14. **Martinez O, Tantral L, Mulherkar N, Chandran K, Basler CF.** 2011. Impact of Ebola mucin-like domain on antiglycoprotein antibody responses induced by Ebola virus-like particles. J Infect Dis **204**(Suppl 3)**:** S825–S832. http://dx.doi.org/10.1093/infdis/jir295.
15. **Bavari S, Bosio CM, Wiegand E, Ruthel G, Will AB, Geisbert TW, Hevey M, Schmaljohn C, Schmaljohn A, Aman MJ.** 2002. Lipid raft microdomains: a gateway for compartmentalized trafficking of Ebola and Marburg viruses. J Exp Med **195:**593–602. http://dx.doi.org/10.1084/jem.20011500.
16. **Warfield KL, Swenson DL, Olinger GG, Kalina WV, Aman MJ, Bavari S.** 2007. Ebola virus-like particle-based vaccine protects nonhuman primates against lethal Ebola virus challenge. J Infect Dis **196**(Suppl 2)**:**S430–S437. http://dx.doi.org/10.1086/520583.
17. **Ye L, Lin J, Sun Y, Bennouna S, Lo M, Wu Q, Bu Z, Pulendran B, Compans RW, Yang C.** 2006. Ebola virus-like particles produced in insect cells exhibit dendritic cell stimulating activity and induce neutralizing antibodies. Virology **351:**260–270. http://dx.doi.org/10.1016/j.virol.2006.03.021.
18. **Manicassamy B, Rong L.** 2009. Expression of Ebolavirus glycoprotein on the target cells enhances viral entry. Virol J **6:**75. http://dx.doi.org/10.1186/1743-422X-6-75.
19. **Hoenen T, Watt A, Mora A, Feldmann H.** 2014. Modeling the lifecycle of Ebola virus under biosafety level 2 conditions with virus-like particles containing tetracistronic minigenomes. J Vis Exp **91:**52381. http://dx.doi.org/10.3791/52381.
20. **Adu-Gyamfi E, Digman MA, Gratton E, Stahelin RV.** 2012. Single-particle tracking demonstrates that actin coordinates the movement of the Ebola virus matrix protein. Biophys J **103:**L41–L43. http://dx.doi.org/10.1016/j.bpj.2012.09.026.
21. **Han Z, Harty RN.** 2005. Packaging of actin into Ebola virus VLPs. Virol J **2:**92. http://dx.doi.org/10.1186/1743-422X-2-92.
22. **McCarthy SE, Licata JM, Harty RN.** 2006. A luciferase-based budding assay for Ebola virus. J Virol Methods **137:**115–119. http://dx.doi.org/10.1016/j.jviromet.2006.06.007.
23. **Hart MK, Wilson JA, Schmaljohn AL.** October 2003. Monoclonal antibodies to Ebola glycoprotein. US patent 6,630,144 B1.
24. **Tong Y, Zhu Y, Xia X, Liu Y, Feng Y, Hua X, Chen Z, Ding H, Gao L, Wang Y, Feitelson MA, Zhao P, Qi ZT.** 2011. Tupaia CD81, SR-BI, claudin-1, and occludin support hepatitis C virus infection. J Virol **85:** 2793–2802. http://dx.doi.org/10.1128/JVI.01818-10.
25. **Shalem O, Sanjana NE, Hartenian E, Shi X, Scott DA, Mikkelsen TS, Heckl D, Ebert BL, Root DE, Doench JG, Zhang F.** 2014. Genome-scale CRISPR-Cas9 knockout screening in human cells. Science **343:**84–87. http://dx.doi.org/10.1126/science.1247005.
26. **Noda T, Sagara H, Suzuki E, Takada A, Kida H, Kawaoka Y.** 2002. Ebola virus VP40 drives the formation of virus-like filamentous particles along with GP. J Virol **76:**4855–4865. http://dx.doi.org/10.1128/JVI.76.10.4855-4865.2002.
27. **Licata JM, Johnson RF, Han Z, Harty RN.** 2004. Contribution of Ebola virus glycoprotein, nucleoprotein, and VP24 to budding of VP40 virus-like particles. J Virol **78:**7344–7351. http://dx.doi.org/10.1128/JVI.78.14.7344-7351.2004.
28. **Johnson RF, Bell P, Harty RN.** 2006. Effect of Ebola virus proteins GP, NP and VP35 on VP40 VLP morphology. Virol J **3:**31. http://dx.doi.org/10.1186/1743-422X-3-31.
29. **Bharat TA, Noda T, Riches JD, Kraehling V, Kolesnikova L, Becker S, Kawaoka Y, Briggs JA.** 2012. Structural dissection of Ebola virus and its assembly determinants using cryo-electron tomography. Proc Natl Acad Sci U S A **109:**4275–4280. http://dx.doi.org/10.1073/pnas.1120453109.
30. **Yang ZY, Duckers HJ, Sullivan NJ, Sanchez A, Nabel EG, Nabel GJ.** 2000. Identification of the Ebola virus glycoprotein as the main viral determinant of vascular cell cytotoxicity and injury. Nat Med **6:**886–889. http://dx.doi.org/10.1038/78645.
31. **Ellis DS, Simpson IH, Francis DP, Knobloch J, Bowen ET, Lolik P, Deng IM.** 1978. Ultrastructure of Ebola virus particles in human liver. J Clin Pathol **31:**201–208. http://dx.doi.org/10.1136/jcp.31.3.201.
32. **Welsch S, Kolesnikova L, Krahling V, Riches JD, Becker S, Briggs JA.** 2010. Electron tomography reveals the steps in filovirus budding. PLoS Pathog **6:**e1000875. http://dx.doi.org/10.1371/journal.ppat.1000875.
33. **Aleksandrowicz P, Marzi A, Biedenkopf N, Beimforde N, Becker S, Hoenen T, Feldmann H, Schnittler HJ.** 2011. Ebola virus enters host cells by macropinocytosis and clathrin-mediated endocytosis. J Infect Dis **204**(Suppl 3)**:**S957–S967. http://dx.doi.org/10.1093/infdis/jir326.
34. **Mingo RM, Simmons JA, Shoemaker CJ, Nelson EA, Schornberg KL, D'Souza RS, Casanova JE, White JM.** 2015. Ebola virus and severe acute respiratory syndrome coronavirus display late cell entry kinetics: evidence that transport to NPC1+ endolysosomes is a rate-defining step. J Virol **89:**2931–2943. http://dx.doi.org/10.1128/JVI.03398-14.
35. **Saeed MF, Kolokoltsov AA, Albrecht T, Davey RA.** 2010. Cellular entry of Ebola virus involves uptake by a macropinocytosis-like mechanism and subsequent trafficking through early and late endosomes. PLoS Pathog **6:**e1001110. http://dx.doi.org/10.1371/journal.ppat.1001110.
36. **Martinez O, Ndungo E, Tantral L, Miller EH, Leung LW, Chandran K, Basler CF.** 2013. A mutation in the Ebola virus envelope glycoprotein restricts viral entry in a host species- and cell-type-specific manner. J Virol **87:**3324–3334. http://dx.doi.org/10.1128/JVI.01598-12.
37. **Nanbo A, Imai M, Watanabe S, Noda T, Takahashi K, Neumann G, Halfmann P, Kawaoka Y.** 2010. Ebolavirus is internalized into host cells via macropinocytosis in a viral glycoprotein-dependent manner. PLoS Pathog **6:**e1001121. http://dx.doi.org/10.1371/journal.ppat.1001121.
38. **Ilinykh PA, Shen X, Flyak AI, Kuzmina N, Ksiazek TG, Crowe JE, Jr, Bukreyev A.** 2016. Chimeric filoviruses for identification and characterization of monoclonal antibodies. J Virol **90:**3890–3901. http://dx.doi.org/10.1128/JVI.00101-16.
39. **Geisbert TW, Strong JE, Feldmann H.** 2015. Considerations in the use of nonhuman primate models of Ebola virus and Marburg virus infection. J Infect Dis **212**(Suppl 2)**:**S91–S97. http://dx.doi.org/10.1093/infdis/jiv284.
40. **Nakayama E, Saijo M.** 2013. Animal models for Ebola and Marburg virus infections. Front Microbiol **4:**267. http://dx.doi.org/10.3389/fmicb.2013.00267.
41. **Hoenen T, Groseth A, Falzarano D, Feldmann H.** 2006. Ebola virus: unravelling pathogenesis to combat a deadly disease. Trends Mol Med **12:**206–215. http://dx.doi.org/10.1016/j.molmed.2006.03.006.
42. **Bray M, Davis K, Geisbert T, Schmaljohn C, Huggins J.** 1999. A mouse model for evaluation of prophylaxis and therapy of Ebola hemorrhagic fever. J Infect Dis **179**(Suppl 1)**:**S248–S258. http://dx.doi.org/10.1086/514292.
43. **Becker S, Spiess M, Klenk HD.** 1995. The asialoglycoprotein receptor is a potential liver-specific receptor for Marburg virus. J Gen Virol **76:**393–399. http://dx.doi.org/10.1099/0022-1317-76-2-393.
44. **Alvarez CP, Lasala F, Carrillo J, Muniz O, Corbi AL, Delgado R.** 2002. C-type lectins DC-SIGN and L-SIGN mediate cellular entry by Ebola virus in cis and in trans. J Virol **76:**6841–6844. http://dx.doi.org/10.1128/JVI.76.13.6841-6844.2002.
45. **Gramberg T, Hofmann H, Moller P, Lalor PF, Marzi A, Geier M, Krumbiegel M, Winkler T, Kirchhoff F, Adams DH, Becker S, Munch J, Pohlmann S.** 2005. LSECtin interacts with filovirus glycoproteins and the spike protein of SARS coronavirus. Virology **340:**224–236. http://dx.doi.org/10.1016/j.virol.2005.06.026.
46. **Powlesland AS, Fisch T, Taylor ME, Smith DF, Tissot B, Dell A, Pohlmann S, Drickamer K.** 2008. A novel mechanism for LSECtin binding to Ebola virus surface glycoprotein through truncated glycans. J Biol Chem **283:**593–602. http://dx.doi.org/10.1074/jbc.M706292200.
47. **Barth H, Schafer C, Adah MI, Zhang F, Linhardt RJ, Toyoda H, Kinoshita-Toyoda A, Toida T, Van Kuppevelt TH, Depla E, Von Weizsacker F, Blum HE, Baumert TF.** 2003. Cellular binding of hepatitis C virus envelope glycoprotein E2 requires cell surface heparan sulfate. J Biol Chem **278:**41003–41012. http://dx.doi.org/10.1074/jbc.M302267200.
48. **O'Hearn A, Wang M, Cheng H, Lear-Rooney CM, Koning K, Rumschlag-Booms E, Varhegyi E, Olinger G, Rong L.** 2015. Role of EXT1 and glycosaminoglycans in the early stage of filovirus entry. J Virol **89:**5441–5449. http://dx.doi.org/10.1128/JVI.03689-14.
49. **Leclerc GM, Boockfor FR, Faught WJ, Frawley LS.** 2000. Development of a destabilized firefly luciferase enzyme for measurement of gene expression. Biotechniques **29:**590–591, 594–596, 598.